Available online at www.sciencedirect.com
SCIENCE DIRECT®
Chemical Physics Letters 402 (2005) 514–518
CHEMICAL PHYSICS LETTERS
www.elsevier.com/locate/cplett

Theoretical prediction of new noble-gas molecules OBNgF (Ng = Ar, Kr, and Xe)

Tsun-Yi Lin, Jeng-Bin Hsu, Wei-Ping Hu *

Department of Chemistry and Biochemistry, National Chung Cheng University, San Hsing 160, Chia-Yi, Min-Hsiung, Taiwan 621, Taiwan

Received 21 December 2004
Available online 8 January 2005

Abstract

High-level electronic structure calculation has been performed on the noble-gas molecules OBArF, OBKrF, and OBXeF. The energetics of the two unimolecular dissociation pathways, (1) OBNgF → OB + Ng + F, and (2) OBNgF → OBF + Ng, were also calculated. The B–Ng bonds were calculated to be 1.8–2.2 Å and were found to be covalent in nature. Highly positive charges were assigned to B and Ng atoms and highly negative charges to O and F atoms. Both unimolecular dissociation pathways were found to have high energy barriers (>15 kcal/mol), and thus suggests that OBNgF are dynamically stable species.

1. Introduction

Since their discovery in 1890s by Ramsay and coworkers, the noble-gas elements have been known for their high stability or chemical inertness [1]. The special electronic configurations of the noble gas atoms, or the so-called octet rule, have been used by chemists since early 20th century, and by almost every chemistry textbook today to illustrate the principles of chemical bonding. The first noble-gas compound $XePtF_6$ was discovered by Barlette in 1962 [2]. In the next few years many Xe-containing compounds and the KrF_2 molecule have been experimentally identified [3]. In the last decade, various new noble-gas molecules have been successfully prepared and identified in the noble-gas matrices [4–6]. Most of these molecules are of the HNgY type where Ng is a noble-gas atom and Y is an electronegative atom or group. The first Ar-containing neutral molecule HArF was discovered in 2000 by Räsänen and coworkers [7], and HKrF was identified in 2002 by the same group [8]. At this point, experimentally identified or theoretically predicted stable neutral Ar and Kr compounds are still very limited [9–14]. Koch et al. [15] in their study of helium chemistry have pointed out that beryllium-, boron-, and carbon-containing acceptor molecules are more suitable binding partners for helium due to the presence of low-lying empty orbitals. This may also apply to the chemistry of other noble-gas elements. The noble gas atoms have been predicted to form relatively strong complexes with BeO [15,16], and indeed the Ar, Kr, and Xe complexes have been observed in the infrared spectra [17]. Several molecules containing noble gas–carbon bonds, such as HNgCCH (Ng = Kr, Xe) [18–20], FArCCH [9] have also been observed or predicted. In the current study, we explore the possible chemical bonding between Ar, Kr, and Xe with boron in OBNgF molecules. The O=B– group was chosen because, similar to BeO, it has empty π orbitals for better orbital interaction with noble-gas atoms.

2. Method

The geometry of OBNgF (Ng = Ar, Kr, and Xe) was calculated using the MP2 and CCSD(T) theory with

* Corresponding author. Fax: +886 5 2721040.
E-mail address: chewph@ccu.edu.tw (W.-P. Hu).

0009-2614/$ - see front matter © 2004 Elsevier B.V. All rights reserved.
doi:10.1016/j.cplett.2004.12.090

6-311+G* and aug-cc-pVTZ atomic basis sets. Since Xe is not available in either sets, we used the Stuttgart/Dresden (SDD) basis set with relativistic effective core potential for Xe [21]. To study the stabilities of OBNgF, the structures of the transition states and products on the two unimolecular dissociation pathways: (1) OBNgF → OB + Ng + F, and (2) OBNgF → OBF + Ng were also calculated. The unrestricted methods (UCCSD(T) and UMP2) were used for the open-shell species (F and BO) and the transition states of the first pathway. (The restricted calculation which leads to incorrect dissociation limits for the first pathway is not considered here.) For other species the restricted and unrestricted methods converged to the same results. The electronic structure calculation was performed using the GAUSSIAN 03 program [22].

3. Results

3.1. OBNgF structure

Fig. 1 shows a schematic structure of the OBNgF molecule and Table 1 shows the calculated geometry parameters for OBNgF. The molecular structures were found to be linear in all calculation. The B–Ng bond lengths are more sensitive (than the Ng–F) to the identity of the noble gas. For example, at the CCSD(T)/aug-cc-pVTZ level the B–Ng bond length increases by 0.35 Å from Ng = Ar to Ng = Xe while the Ng–F bond length increases by only 0.12 Å. In comparison, the Ng–F bonds in HArF, HKrF, and HXeF calculated at the same levels are 1.993, 2.041, and 2.129 Å [23], respectively, very similar to the Ng–F bond lengths in OBNgF calculated in the current study. The O–B distance increases only very slightly (~0.004 Å) from Ng = Ar to Ng = Xe.

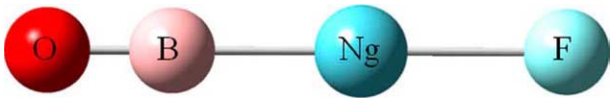

Fig. 1. A schematic structure of OBNgF.

Table 2
Atomic charges[a] calculated at MP2/aug-cc-pVTZ level[b]

		H	Ng	F
HArF		0.18 (0.23)	0.41 (0.53)	−0.59 (−0.76)
HKrF		0.09 (0.11)	0.45 (0.64)	−0.54 (−0.75)
HXeF		0.003 (−0.04)	0.49 (0.81)	−0.49 (−0.77)
	O	B	Ng	F
OBArF	−0.41 (−0.68)	0.54 (0.87)	0.46 (0.56)	−0.59 (−0.75)
OBKrF	−0.41 (−0.70)	0.45 (0.75)	0.50 (0.69)	−0.53 (−0.74)
OBXeF	−0.42 (−0.72)	0.37 (0.61)	0.52 (0.86)	−0.47 (−0.76)

[a] ChelpG charges, values in the parentheses are NBO charges.
[b] Using geometry optimize at CCSD(T)/aug-cc-pVTZ level.

3.2. Charge distribution

The calculated ChelpG and NBO atomic charges of OBNgF at MP2/aug-cc-pVTZ level are listed and compared to those of HNgF in Table 2. In OBNgF both the Ng and B atoms are assigned to very positive charges while the F and O atoms are assigned to very negative charges. In comparison, the hydrogens are assigned to very small charges in HNgF. The Laplacian of the electron density (MP2/aug-cc-pVTZ) at the bond critical points of the B–Ar and B–Kr bonds in OBNgF was calculated to be −0.18 and −0.29 a.u., respectively. The negative values indicate the covalent character of the Ng–B chemical bonding [15,24]. In comparison, the calculated values at the bond critical points of the H–Ar and H–Kr bonds in HNgF were −0.61 and −0.42 a.u., respectively. The contour plots of the valence electron

Table 1
Calculated bond length (in Å) of OBNgF[a]

	MP2/6-311+G*	MP2/aug-cc-pVTZ	CCSD(T)/6-311+G*	CCSD(T)/aug-cc-pVTZ
OBArF				
R(O–B)	1.209	1.213	1.206	1.207
R(B–Ar)	1.806	1.802	1.891	1.827
R(Ar–F)	2.060	1.979	2.058	1.989
OBKrF				
R(O–B)	1.212	1.215	1.207	1.209
R(B–Ar)	1.982	1.953	2.011	1.972
R(Kr–F)	2.062	2.024	2.071	2.031
OBXeF				
R(O–B)	1.214	1.217	1.210	1.211
R(B–Ar)	2.165	2.155	2.191	2.173
R(Xe–F)	2.146	2.116	2.145	2.112

[a] Calculated OBNgF geometries are linear at all levels.

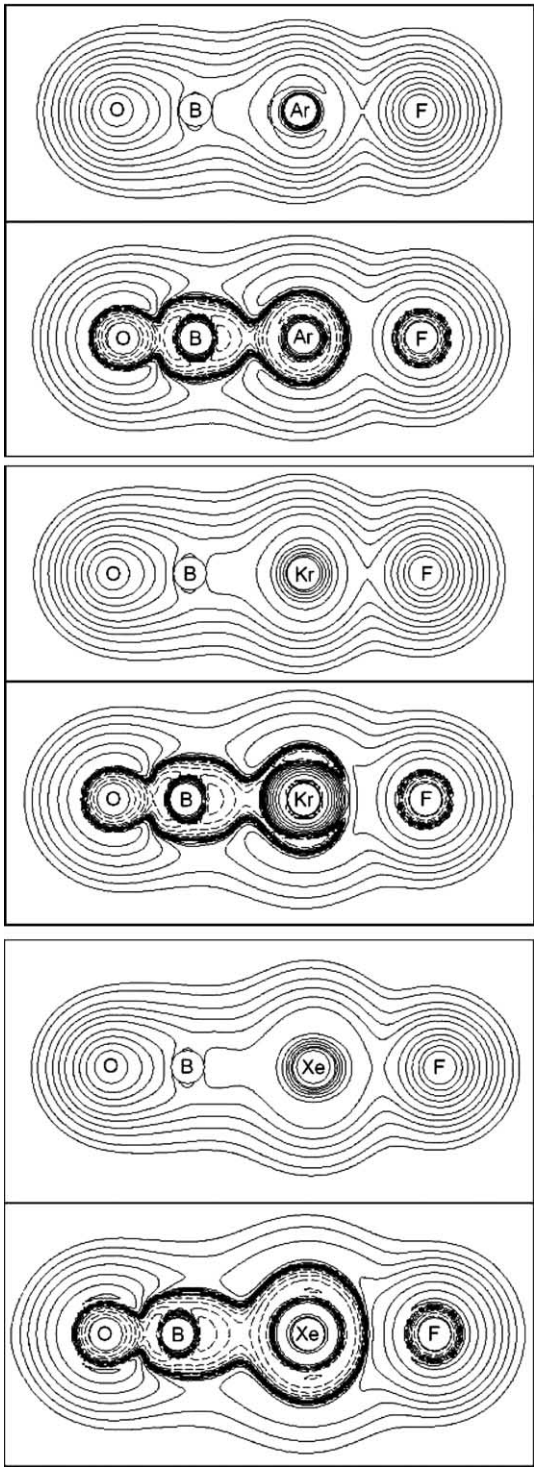

Fig. 2. Contour plots of electron density (upper) and Laplace concentration (lower) calculated at MP2/aug-cc-pVTZ level in which dashed contour lines are in regions of charge concentration and solid lines in regions of charge depletion.

and the Laplacian density of the OBNgF are shown in Fig. 2. The distortion of the contour lines also suggests the covalent characters of the Ng–B bonds, and the ionic characters of the Ng–F bonds.

3.3. Dissociation energetics

The intrinsic stability of the new molecules can be judged by the barrier heights and the energies of reaction of the two unimolecular dissociation pathways [23,25]. The first pathway corresponds to linear dissociation to constituent atoms and radicals and the second pathway corresponds to bending dissociation to the global minimum. The calculated energetics of the two pathways is listed in Table 3. For OBArF the highest-level calculation shows that the first pathway is almost isoergic with a sizable barrier of 14.7 kcal/mol. The second pathways for OBArF is highly exoergic but with a barrier of 18.3 kcal/mol. Table 3 also shows that the calculated energies for the first pathways are sensitive both to the theoretical levels and the atomic basis sets while for the second pathway the energies are less sensitive to the levels of theory.

For OBKrF, the CCSD(T)/aug-cc-pVTZ calculation shows that the first pathway is endoergic by 25.1 kcal/mol. The energy of reaction of the second pathway for OBKrF is −134.5 kcal/mol, ~24 kcal/mol less exoergic than that of OBArF. The energy barrier of the second pathway is 27.6 kcal/mol, ~9 kcal/mol higher than that of OBArF.

For OBXeF, the CCSD(T)/aug-cc-pVTZ calculation shows that the first pathway is endoergic by 49.5 kcal/mol. That is, the sum of the B–Xe and Xe–F bond energies is similar to that of a weak chemical bond. At the CCSD(T) level we found that the energy for the first dissociation pathway is monotonically increasing and the energy barrier is equal to the energy of reaction. The energy of reaction of the second pathway for OBXeF is −110.0 kcal/mol, 25 kcal/mol less exoergic than that of OBKrF. The energy barrier of the second pathway is 35.2 kcal/mol, ~8 kcal/mol higher than that of OBKrF.

Since sizable barriers exist for both dissociation pathways, OBNgF (Ng = Ar, Kr, Xe) are expected to be stable at low temperature environment free of reactive impurities. The related OBHeF and OBNeF molecules were found to have negligible or even nonexistent bending barriers and are thus dynamically unstable.

3.4. Transition state geometry

The calculated geometries of the transition states are shown in Tables 4 and 5. As shown in Tables 1 and 4, at the transition state of the first pathway the B–Ng bond lengths are ~0.5 Å longer and the Ng–F bond lengths ~0.1–0.3 Å longer than those in OBNgF. Thus the dissociation would proceed by first lengthening the B–Ng bond before increasing the Ng–F significantly. While for OBArF the calculated transition state geometry of the first pathway is linear at all levels, the transition state geometry for OBKrF is slightly bent at higher level calculation.

Table 3
Calculated energetics[a] (in kcal/mol) of the two dissociation pathways

	OBNgF → OB + Ng + F		OBNgF → OBF + Ng	
	$V^{\neq}$	Erxn	$V^{\neq}$	Erxn
Ng = Ar				
MP2/6-311+G*	33.8 (32.3)	−7.6 (−10.1)	14.5 (14.3)	−167.4 (−166.8)
MP2/aug-cc-pVTZ	39.5 (38.5)	9.8 (7.0)	17.5 (17.1)	−158.1 (−157.8)
CCSD(T)/6-311+G*	8.1 (7.2)	−13.8 (−16.0)	16.4 (16.6)	−165.8 (−164.7)
CCSD(T)/aug-cc-pVTZ	14.7	0.8	18.3	−158.8
Ng = Kr				
MP2/6-311+G*	37.1 (35.6)	16.1 (13.5)	27.6 (27.2)	−143.6 (−143.0)
MP2/aug-cc-pVTZ	45.6 (43.8)	34.1 (31.4)	26.8 (26.4)	−133.7 (−133.3)
CCSD(T)/6-311+G*	18.5 (16.8)	9.4 (6.9)	28.8 (28.5)	−142.5 (−141.8)
CCSD(T)/aug-cc-pVTZ	26.6[b]	25.1	27.6	−134.5
Ng = Xe				
MP2/6-311+G*	52.7 (50.7)	42.4 (39.9)	33.8 (33.3)	−117.3 (−116.6)
MP2/aug-cc-pVTZ	59.0 (57.0)	57.8 (55.3)	34.1 (33.6)	−110.0 (−109.4)
CCSD(T)/6-311+G*	N.A.[c]	35.2 (32.7)	35.1 (34.7)	−116.8 (−116.1)
CCSD(T)/aug-cc-pVTZ	N.A.[c]	49.5	35.2	−110.0

[a] Born–Oppenheimer energies, values in parentheses including zero-point energies. $V^{\neq}$: barrier height, Erxn: energy of reaction.
[b] Using geometry calculated at CCSD(T)/6-311+G* level.
[c] Transition state not found, see text.

Table 4
Calculated transition state geometries (bond length in Å, angle in degrees) for the OBNgF → OB + Ng + F reaction

	MP2/6-311+G*	MP2/aug-cc-pVTZ	CCSD(T)/6-311+G*	CCSD(T)/aug-cc-pVTZ
Ng = Ar[a]				
R(O–B)	1.204	1.210	1.208	1.212
R(B–Ar)	2.018	2.119	2.161	2.291
R(Ar–F)	1.963	1.929	2.103	2.089
Ng = Kr				
R(O–B)	1.210	1.213	1.212	
R(B–Kr)	2.382	2.485	2.551	
R(Kr–F)	2.103	2.097	2.277	
A(O–B–Kr)	180.0	165.2	155.1	
A(B–Kr–F)	180.0	177.2	176.4	
Ng = Xe				
R(O–B)	1.222	1.222		
R(B–Xe)	3.330	3.386		
R(Xe–F)	2.439	2.419		
A(O–B–Xe)	92.2	88.7		
A(B–Xe–F)	178.3	174.6		

[a] Calculated TS geometries for the OBArF reaction are linear at all levels.

As shown in Tables 1 and 5, at the transition state of the second pathway the B–Ng bond lengths are ~0.1 Å shorter and the Ng–F bond lengths are ~0.2–0.3 Å longer than those in OBNgF. The B–Ng–F angles in the bending transition states are very close to the H–Ng–F angles in the bending transition states of HNgF calculated previously [23,25,26].

4. Summary

We have made correlated extended-basis-set calculation on the OBArF, OBKrF, and OBXeF molecules and on the energetics for their dissociation pathways. The B–Ng bonds in OBNgF were calculated to be 1.8–2.2 Å and were found to be covalent in nature. The calculated results suggest that these molecules might be dynamically stable from unimolecular dissociation and could be targets for future experimental identification, although new synthesis techniques different from those for HNgF may need to be devised.

Acknowledgements

This work is supported by the National Science Council of Taiwan. We are grateful to the National Center for High-Performance Computing (NCHC) of Taiwan for providing part of the computational resources.

Table 5
Calculated transition state geometries (bond length in Å, angle in degrees) for the OBNgF → OBF + Ng reaction

	MP2/6-311+G*	MP2/aug-cc-pVTZ	CCSD(T)/6-311+G**	CCSD(T)/aug-cc-pVTZ
Ng = Ar				
R(O–B)	1.205	1.209	1.200	1.204
R(B–Ar)	1.710	1.704	1.718	1.709
R(Ar–F)	2.292	2.203	2.291	2.207
A(O–B–Ar)	178.0	178.6	178.4	178.6
A(B–Ar–F)	111.5	109.5	110.3	108.9
Ng = Kr				
R(O–B)	1.207	1.211	1.203	1.205
R(B–Kr)	1.863	1.840	1.869	1.847
R(Kr–F)	2.335	2.270	2.337	2.275
A(O–B–Kr)	177.4	178.1	177.6	178.2
A(B–Kr–F)	102.6	102.2	101.9	102.1
Ng = Xe				
R(O–B)	1.211	1.214	1.206	1.209
R(B–Xe)	2.040	2.032	2.053	2.041
R(Xe–F)	2.384	2.339	2.387	2.343
A(O–B–Xe)	178.0	178.2	177.9	178.0
A(B–Xe–F)	98.0	98.1	98.1	98.4

References

[1] N.N. Greenwood, A. Earnshaw, Chemistry of the Elements, Butterworth-Heinemann, Oxford, 2001.
[2] N. Bartlett, Proc. Chem. Soc. (1962) 218.
[3] D.T. Hawkins, W.E. Falconer, N. Bartlett, Noble-Gas Compounds. A Bibliography: 1962–1976, IFI/Plenum, New York, 1978.
[4] M. Pettersson, J. Lundell, M. Räsänen, J. Chem. Phys. 102 (1995) 6423.
[5] M. Pettersson, J. Lundell, M. Räsänen, J. Chem. Phys. 103 (1995) 205.
[6] M. Pettersson, J. Lundell, L. Khriachtchev, M. Räsänen, J. Chem. Phys. 109 (1998) 618.
[7] L. Khriachtchev, M. Pettersson, N. Runeberg, J. Lundell, M. Räsänen, Nature 406 (2000) 874.
[8] M. Pettersson, L. Khriachtchev, A. Lignell, M. Räsänen, J. Chem. Phys. 116 (2002) 2508.
[9] A. Cohen, J. Lundell, R.B. Gerber, J. Chem. Phys. 119 (2003) 6415.
[10] P. Antoniotti, N. Bronzolino, F. Grandinetti, J. Phys. Chem. A 107 (2003) 2974.
[11] B. Liang, L. Andrews, J. Li, B.E. Bursten, Inorg. Chem. 43 (2004) 882.
[12] S. Borocci, N. Bronzolino, F. Grandinetti, Chem. Phys. Lett. 384 (2004) 25.
[13] M. Pettersson, J. Lundell, M. Räsänen, Eur. J. Inorg. Chem. (1999) 729.
[14] S. Yockel, J.J. Seals III, A.K. Wilson, Chem. Phys. Lett. 393 (2004) 448.
[15] W. Koch, G. Frenking, J. Gauss, D. Cremer, J.R. Collins, J. Am. Chem. Soc. 109 (1987) 5917.
[16] G. Frenking, W. Koch, J. Gauss, D. Cremer, J. Am. Chem. Soc. 110 (1988) 8007.
[17] C.A. Thompson, L. Andrews, J. Am. Chem. Soc. 116 (1994) 423.
[18] H. Tanskanen, J. Lundell, M. Pettersson, H. Kiljunen, M. Räsänen, J. Am. Chem. Soc. 125 (2003) 4696.
[19] V.I. Feldman, F.F. Sukhov, A.Y. Orlov, I.V. Tyulpina, J. Am. Chem. Soc. 125 (2003) 4698.
[20] L. Khriachtchev, H. Tanskanen, A. Cohen, R.B. Gerber, J. Lundell, M. Pettersson, H. Kiljunen, M. Räsänen, J. Am. Chem. Soc. 125 (2003) 6876.
[21] A. Nicklass, M. Dolg, H. Stoll, H. Preuss, J. Chem. Phys. 102 (1995) 8942.
[22] M.J. Frisch et al., GAUSSIAN 03, Revision B.04, Gaussian, Inc, Pittsburgh, PA, 2003.
[23] Y.-L. Chen, W.-P. Hu, J. Phys. Chem. A 108 (2004) 4449.
[24] M.W. Wong, J. Am. Chem. Soc. 122 (2000) 6289.
[25] G.M. Chaban, J. Lundell, R.B. Gerber, Chem. Phys. Lett. 364 (2002) 628.
[26] S.-Y. Yen, C.-H. Mou, W.-P. Hu, Chem. Phys. Lett. 383 (2004) 606.